Dissociation Enthalpies of Synthesized Multicomponent Gas Hydrates with Respect to the Guest Composition and Cage Occupancy

Marisa B. Rydzy, Judith M. Schicks,* Rudolf Naumann, and Jörg Erzinger

GeoForschungsZentrum Potsdam, Telegrafenberg, 14473 Potsdam, Germany

Received: February 14, 2007; In Final Form: May 25, 2007

This study presents the influences of additional guest molecules such as C_2H_6, C_3H_8, and CO_2 on methane hydrates regarding their thermal behavior. For this purpose, the onset temperatures of decomposition as well as the enthalpies of dissociation were determined for synthesized multicomponent gas hydrates in the range of 173−290 K at atmospheric pressure using a Calvet heat-flow calorimeter. Furthermore, the structures and the compositions of the hydrates were obtained using X-ray diffraction and Raman spectroscopy as well as hydrate prediction program calculations. It is shown that the onset temperature of decomposition of both sI and sII hydrates tends to increase with an increasing number of larger guest molecules than methane occupying the large cavities. The results of the calorimetric measurements also indicate that the molar dissociation enthalpy depends on the guest-to-cavity size ratio and the actual concentration of the guest occupying the large cavities of the hydrate. To our knowledge, this is the first study that observes this behavior using calorimetrical measurements on mixed gas hydrates at these temperature and pressure conditions.

1. Introduction

Clathrate hydrates are nonstoichiometric icelike crystalline solids composed of a three-dimensional network of hydrogen-bonded water molecules that confines guest molecules in well-defined cavities of different sizes. These clathrate hydrates, better known as gas hydrates, have generated considerable interest because the occurrence of large reserves of natural gas present as clathrate hydrates in permafrost regions and beneath the seafloor has been reported.[1,2] Not only may gas hydrates serve as a significant hydrocarbon source but also, because their stability reacts sensitively to changes in pressure and temperature, gas hydrates in sediments may impact global climate and seafloor stability. An understanding of thermophysical properties such as heat capacity, thermal conductivity, or dissociation enthalpies will be required to develop production schemes that can be used to recover natural gas from hydrate deposits and to predict the role of natural gas hydrates regarding climate change.

There are three common gas hydrates structures capable of holding light hydrocarbons. These structures vary in the ratio of small and large cavities as shown in Table 1. Generally, small molecules such as methane and ethane form structure I hydrates. Larger molecules such as propane or isobutene form structure II hydrates with the small cavities empty. Even larger molecules such as isopentane are known to form structure H hydrates in the presence of a help gas such as methane.

This study is concerned mainly with the investigation of enthalpies of gas hydrate dissociation. The dissociation enthalpy is defined as the enthalpy change to decompose the gas hydrate. Two types of gas hydrate dissociation are generally distinguished: the decomposition of gas hydrates into ice and gas, and the decomposition into gas and liquid. The difference in enthalpy between both reactions is assumed to be equal to the enthalpy of fusion of ice (n·H_2O).[3]

TABLE 1: Number of Cavities Per Unit Cell for the Different Gas Hydrate Structures

	cavities				
	5^{12}	$5^{12}6^2$	$5^{12}6^4$	$4^35^66^3$	$5^{12}6^8$
sI	2	6			
sII	16		8		
sH	3			2	1

According to Sloan,[2] to a first approximation the dissociation enthalpy is a function of the following factors: the hydrogen bonds making up the lattice, the cavity occupation, and the guest size. Long[4] suggested that about 80% of the total dissociation enthalpy is due to the strength of the water hydrogen bonds. Therefore, it can be assumed that a higher energy is required to dissociate one unit cell of structure II hydrate comprising 136 water molecules than to decompose one unit cell of structure I hydrate, which is made up of only 46 water molecules.

Moreover, it is hypothesized that the dissociation enthalpy depends on the cage occupancy,[5] at least regarding the large cages. When more large cavities are occupied (irrespective of type of guest molecule), the hydrate lattice is more stable. Handa[6,7] performed calorimetric measurements on single component gas hydrates that showed this impact of cage occupancy on the dissociation enthalpy.

Another key to qualitatively understanding gas hydrate stability is the diameter of the guest molecule with respect to the diameter of the cavity (the guest-to-cavity size ratio).[2] Guest-to-cavity size ratios for different guest molecules are listed in Table 2. The dissociation enthalpy reflects the magnitude of stabilization due to the interactions between guest and host. It is hypothesized that the guest molecules prevent interactions between opposite water molecules and thereby inhibit the lattice from collapsing. It is reasonable to assume that an increase in guest size increases the shielding function of the guest, thus resulting in a higher stability. However, if the size of the guest molecules becomes too large the stability of the cavities

* Corresponding author. Telephone: +49-331-288-1487. Fax: +49-331-288-1436. E-mail: Schick@gfz-potsdam.de.

10.1021/jp0712755 CCC: $37.00
Published on Web 07/20/2007

TABLE 2: Ratios of Molecular Diameters to Cavity Diameters for Some Guest Molecules[2]

		guest-to-cavity diameter ratio			
guest molecule	guest diameter (Å)	for guest in 5^{12} of sI	for guest in $5^{12}6^2$ of sI	for guest in 5^{12} of sII	for guest in $5^{12}6^4$ of sII
CH_4	4.36	0.855	0.744	0.868	0.655
CO_2	5.12	1.0	0.834	1.02	0.769
C_2H_6	5.50	1.08	0.939	1.10	0.826
C_3H_8	6.28	1.23	1.07	1.25	0.943

decreases because of the repulsive forces between the guest and the water molecules of the lattice.[8]

The *molar* dissociation enthalpy, the change in enthalpy to decompose 1 mol of $M\cdot(H_2O)_n$, can be estimated to a first-order approximation from phase equilibrium data plotted in a Clausius−Clapeyron plot (semilogarithmic plots of pressure versus the reciprocal temperature). The slope of the dissociation lines in this plot [d ln(P)/d(1/T)] gives $\Delta h_d'$ by applying the Clausius−Clapeyron equation:

$$\frac{\mathrm{d}\ln(P)}{\mathrm{d}(1/T)} = -\frac{\Delta h_d'}{z\cdot R} \tag{1}$$

where R is the universal gas constant ($R = 8.31451$ J/K·mol) and z is the compressibility of the respective guest gas and ranges about 1 at low temperatures.[9]

Sloan and Fleyfel[10] calculated the molar dissociation enthalpies of various single and binary guest hydrates using the Clausius−Clapeyron equation (eq 1). From their results, Sloan and Fleyfel concluded that it is possible, to a first approximation, to determine the dissociation enthalpy by knowing the size of the guest molecule and thus the type of cavities occupied. Furthermore, they showed the independence of the dissociation enthalpy from the concentration of the guest gas in the case of gas mixtures. Skovborg and Rasmussen[11] questioned the approach of Sloan and Fleyfel, arguing that their theory does not seem to be valid, because they did not take into account the amounts of water entering the hydrate structure per mole of different gases. For example, pure propane occupies only the large cavities of structure II hydrates, thus resulting in a higher number of water molecules (n) per mole of gas and consequently in a higher enthalpy compared to that of a propane−methane mixture, where both cavities are potentially filled.

In this study, differential scanning calorimetry (DSC) was performed on synthesized gas hydrates to investigate how the incorporation of additional guest molecules, such as C_2H_6, C_3H_8, and CO_2, influences dissociation enthalpies and onset temperatures of decomposition of methane hydrates. The measurements were conducted systematically with respect to the gas composition, structure, and hydrate/ice ratio of the multicomponent gas hydrates.

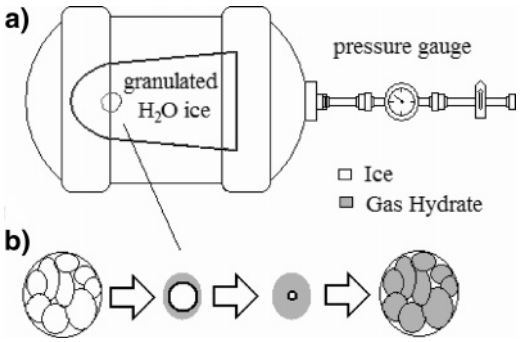

Figure 1. Gas hydrate formation apparatus: (a) High-pressure reaction vessel, (b) gas hydrate formation process from ice and gas to gas hydrate.

TABLE 3: Composition of the Hydrate-Forming Feed Gas and Hydrate Formation Conditions

gas	CH_4	CO_2	C_2H_6	C_3H_8	P (MPa)	T (K)
mixture 1	1.00				15	271
mixture 2	0.95	0.05			10	273
mixture 3	0.90	0.10			10	273
mixture 4	0.90		0.05	0.05	5	271
mixture 5	0.98		0.01	0.01	6	271

2. Experimental Section

2.1. Sample Preparation. The gas hydrate samples were synthesized by using the following procedure. Powdered ice was created by spraying deionized water into liquid nitrogen. To make sure that all liquid nitrogen vaporized completely, the ice was stored for several hours at a temperature of about 271 K. Afterward, approximately 100 g of the ice was loaded into a high-pressure reaction vessel (Figure 1) that was closed and pressurized with the preferred gas mixture. The vessel itself contained a volume of approximately 1.1 L and was pressure-resistant up to 400 bar. The gas mixtures used in our experiments as well as the formation conditions (pressures and temperatures) are listed in Table 3. The gas mixtures were certified gas mixtures and were purchased from Air Liquid, former Messer Griesheim GmbH in Schwante, Germany. The pressurized samples were stored at the respective temperatures and pressures (Table 3) over several weeks until no more changes in pressure were observed. The samples were recovered from the accumulators in a climate chamber at atmospheric pressure and temperatures of approximately 260 K and stored immediately in liquid nitrogen. Before analyses, the gas hydrate samples were prepared in liquid nitrogen inside a nitrogen-flooded cooled glovebox as hereafter described. Care was taken that the hydrate sample itself was always placed in liquid nitrogen to avoid alteration due to early dissociation. The samples consisted of both ice and gas hydrates. According to the following X-ray diffraction measurements, the content of hydrate in the samples varied between 50 and 60%. The distribution of these components in the sample was usually very heterogeneous. To attain an even distribution of these components in each specimen, the samples had been ground and stirred thoroughly with the SPEX Certi Prep 6750 Freezer Mill at 77 K. A defined amount of the fine-grained material was filled into an aluminum crucible (7-mm diameter, 11-mm long), which was then sealed with a drilled aluminum cover. The residual pulverized material was investigated using X-ray power diffractometry to determine the gas hydrate structure, as well as the hydrate/ice ratio (section 2.3). The samples to be measured with the DSC were weighed with a Leco 150 precision balance, which was also located inside the glovebox. The balance has an internal error of ±0.001 mg. Approximately 150 mg of gas hydrate was filled into each crucible. The so prepared samples were stored in liquid nitrogen until the measurements were performed.

2.2. Experimental Setup: Differential Scanning Calorimetry. The calorimetric measurements were carried out with a SETARAM Calvet DSC 121. The measuring device was made up of two refractory sintered alumina tubes crossing a heating metal block from side to side. One was the reference tube, the

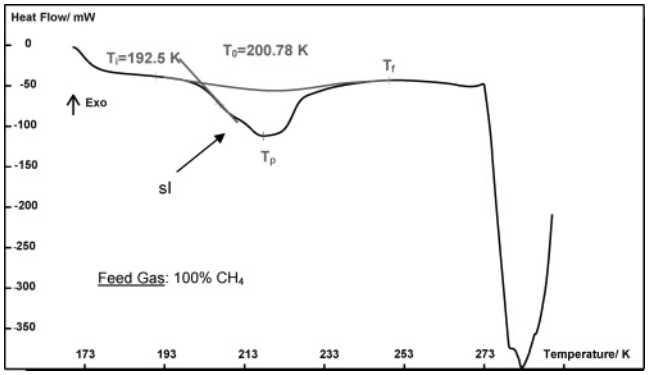

Figure 2. DSC thermogram obtained for the dissociation of gas hydrates synthesized with Mixture 1.

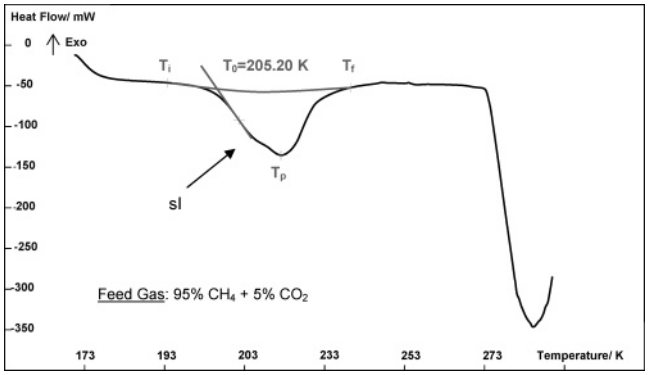

Figure 3. DSC thermogram obtained for the dissociation of gas hydrates synthesized with Mixture 2.

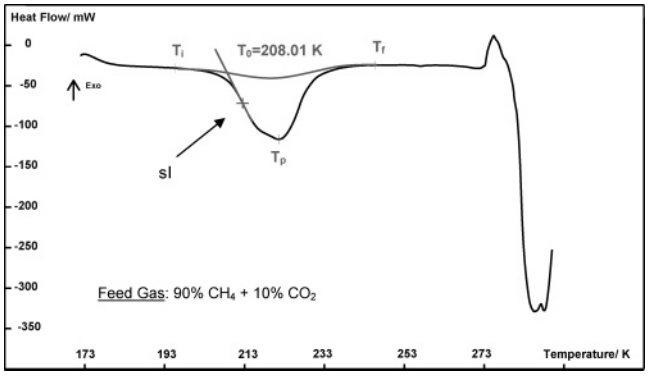

Figure 4. DSC thermogram obtained for the dissociation of gas hydrates synthesized with Mixture 3.

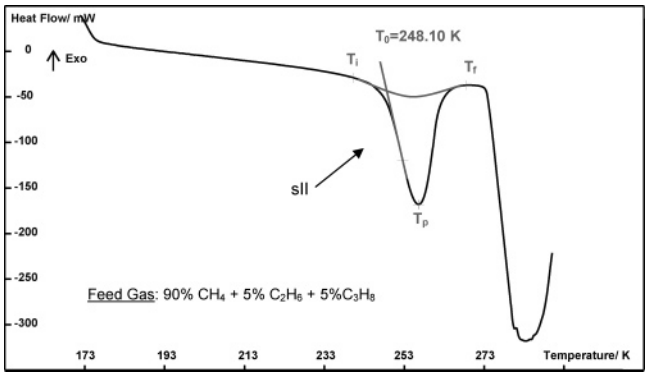

Figure 5. DSC thermogram obtained for the dissociation of gas hydrates synthesized with Mixture 4.

other the measuring tube. The crucible containing the sample or reference material could be introduced from either side of the tubes and was then slid into the sensitive measurement zone. Two oppositely connected thermopiles were wrapped around the central area of the tubes and fitted into the calorimetric block to measure the differential heat signal between sample and reference tube. Linear increase of the furnace temperature as well as signal acquisition, amplification, conversion, and transfer of the signal were computer controlled.

Caloric calibration of the DSC 121 instrument as defined by SETARAM was checked with indium (NIST Standard). Temperature calibration measurements were performed using indium, tin, and gallium. The uncertainties for the results of enthalpy and temperature measurements were ±1% rel. and ±0.02 K, respectively.

To perform calorimetric measurements on gas hydrates under atmospheric conditions, subambient cooling of the calorimetric block was required. This was provided by the use of liquid nitrogen in an external cooling device. To avoid early dissociation of the gas hydrate sample, the calorimetric block was cooled to 173 K. The sample was then introduced into the calorimeter, and the particular heating program was started.

The heating program for enthalpy determination consisted of a linear increase of furnace temperature from 173.15 to 293.15 K with a heating rate of 5 K/min, which was enclosed by two isothermal sequences with a duration of 150 s. Three measurements were conducted for each system listed in Table 3.

2.3. Experimental Setup: X-ray Diffractometry and Raman Spectroscopy. X-ray diffraction applied with a cryo cell was used for the identification of hydrate phases and determination of the hydrate structure and the ice-to-hydrate ratio. The diffraction patterns of the gas hydrate samples were obtained with a Siemens D5000 powder diffractometer employing a Cu tube and a graphite monochromator. The diffraction data were collected from 8 to 51° 2θ with a step width of 0.02° and a counting time of 2 s per step. The generator settings were 40 KV and 30 mA. The Rietveld algorithm BGMN was used for refinement and quantitative phase determination.[12]

In addition, the samples were analyzed with a confocal Raman spectrometer (LABRAM, HORIBA JOBIN YVON), which allowed the laser beam to be focused on a precise point, thus ensuring that only the selected phase was analyzed.

3. Results and Discussion

Figures 2−6 show the heat flow versus temperature curves obtained through differential scanning calorimetry. The DSC traces show signals for endothermic phase transitions expected in the temperature zone of ice melting and gas hydrate dissociation. The dominant peak occurring in all figures at about 273 K is associated with the melting of ice.

The endothermic event in the measuring curve depicted in Figure 2 at a temperature of 201 K represents the dissociation of the gas hydrates formed from pure methane (Mixture 1). Likewise, the dissociation of the binary gas hydrate systems of Mixtures 2 and 3 is represented by the endothermic peaks in Figures 3 and 4 at 205 and 208 K, respectively. X-ray powder diffractometry (XRPD) measurement determined that the three samples are composed of ice and structure I hydrate, which was expected because CH_4 and CO_2 form structure I hydrates.

The endothermic behavior at 248 K shown in Figure 5 represents the decomposition of gas hydrates formed from 90% CH_4, 5% C_2H_6, and 5% C_3H_8 (Mixture 4). According to X-ray diffraction measurements, the gas hydrates are composed of structure II, which, again, was expected because gas mixtures containing propane greater than one percent typically form structure II hydrates.[2] The increase in gas hydrate stability

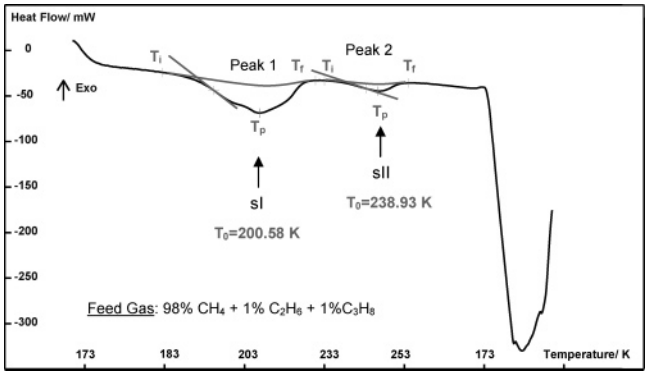

Figure 6. DSC thermogram obtained for the dissociation of gas hydrates synthesized with Mixture 5.

compared to that of the structure I hydrates corresponds well to observations made by Collett.[13]

In contrast to the behavior of the previous systems (Mixtures1−4), the dissociation of the gas hydrates formed from 98% CH_4, 1% C_2H_6, and 1% C_3H_8 (Mixture 5) resulted in two endothermic peaks, as shown in the DSC trace in Figure 6. This implies the coexistence of two gas hydrate phases. X-ray diffraction measurements confirmed the presence of both structure I and structure II hydrates. The bigger, broader peak (Peak 1) occurs at a lower onset temperature of 201 K, which corresponds to the onset temperature of the dissociation of pure methane hydrate (Figure 2). Therefore, Peak 1 can be assumed to represent the dissociation of structure I hydrates, containing methane and probably ethane. The smaller peak (Peak 2) occurs at a higher temperature which corresponds to dissociation of structure II hydrates (in Figure 5) and is assumed to represent the decomposition of structure II hydrates, containing methane, ethane, and propane.

To sum it up, it can be said that a gas composition of 98% CH_4, 1% C_2H_6, and 1% C_3H_8 (Mixture 5) results in the formation of two coexisting hydrate phases composed of structures I and II, whereas a gas mixture of 90% CH_4, 5% C_2H_6, and 5% C_3H_8 (Mixture 4) forms as one single phase of structure II hydrates. The coexistence of structure I and structure II hydrates, synthesized from Mixture 5 at similar p-T conditions, was recently reported by Schicks et al.[14] Propane is known to fit in the large cages in structure II hydrates only, whereas methane and ethane are known to form structure I hydrates with C_2H_6 occupying only large cages and CH_4 occupying both small and large cages.[2] Subramanian et al. observed the formation of sII hydrates in binary systems of sI formers CH_4 and C_2H_6 in the case when the C_2H_6 fraction is small.[15,16] The composition at which, at a certain temperature and pressure, the methane−ethane hydrates show a structural transition from sI to sII is referred to as the "lower transitional point".[15] Because pure methane, situated at one of the extremes of the composition range, forms sI hydrates, the structure of methane−ethane hydrates must revert from sII to sI, as the CH_4 contents approaches 100% ("upper transitional point").[16] Furthermore, sI and sII hydrates are assumed to coexist close to the upper and lower transition points.

A distinctive feature of the dissociation peaks of the synthetic gas hydrates composed of structure I (Figures 2−4 and 6) is the change in steepness of the descending slope at 213 K. This change represents a decrease in the dissociation rate, which is likely due to the formation of an ice layer, which encloses the sample and was formed from dissociated gas hydrate. This layer hinders gas diffusion but does not avert it totally. A similar observation was described by Stern et al.[17] as the self-preservation effect of methane hydrates. It should be noted that no change in dissociation rate occurs for the structure II hydrates (Figures 5 and 6). Stern et al.[17] already suggested that the extent of the preservation effect may differ considerably for some structure II hydrates because of a significantly higher dissociation temperature compared to that of methane hydrate. One might assume that the ice resulting from the dissociating structure II hydrates forms more slowly than the ice resulting from the dissociation of structure I hydrates, because the dissociation temperature of the structure II hydrate is closer to the ice melting point. Furthermore, it might be suggested that the guest molecule inside the hydrate lattice of structure II hydrate has, at the point of hydrate dissociation, a larger molecular kinetic energy because of the higher dissociation temperature of structure II hydrates. Therefore, it can be concluded that it becomes easier for the guest molecule to diffuse as the temperature increases.

TABLE 4: Onset Temperatures of Decomposition (T_0) and Standard Deviations (s_T)

sample	T_0 (K)	s_T (K)
mixture 1 sI	200.78	0.29
mixture 2 sI	205.20	0.20
mixture 3 sI	208.01	0.40
mixture 4 sII	248.10	0.17
mixture 5 sI	200.58	0.43
mixture 5 sII	238.93	1.77

TABLE 5: Enthalpy of Decomposition in Ice and Gas (Δh_d) and Standard Deviations (s_T)

sample	Δh_d (J/g)	$s_{\Delta h}$ (J/g)
mixture 1 sI	125.4	3.0
mixture 2 sI	134.8	5.3
mixture 3 sI	127.7	7.0
mixture 4 sII	292.4	11.6
mixture 5 sI	262.7	7.1
mixture 5 sII	264.4	8.2

3.1. Onset Temperature of Gas Hydrate Decomposition. The onset temperatures of decomposition (T_0) and their standard deviations (s_T) for the gas hydrates formed from either pure CH_4 or gas mixtures are given in Table 4. To construct the onset point of a phase transition in a DSC curve, the inflectional tangent at the ascending peak slope is extended until it intersects the extrapolated initial baseline (Figure 7). The point of intersection is the onset point at the designated onset temperature. Note that T_0 does not represent the actual beginning of the phase transition but is the most reproducible point. The actual beginning of the gas hydrate dissociation is actually established by the initial peak temperature (T_i), which marks the first deviation of the measuring curve from the baseline and which is not reproducible.[18] T_i obtained for methane hydrate (Figures

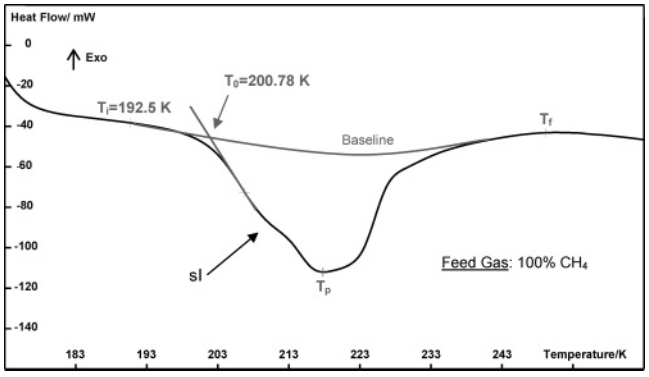

Figure 7. Determination of onset temperature T_0 of Mixture 1.

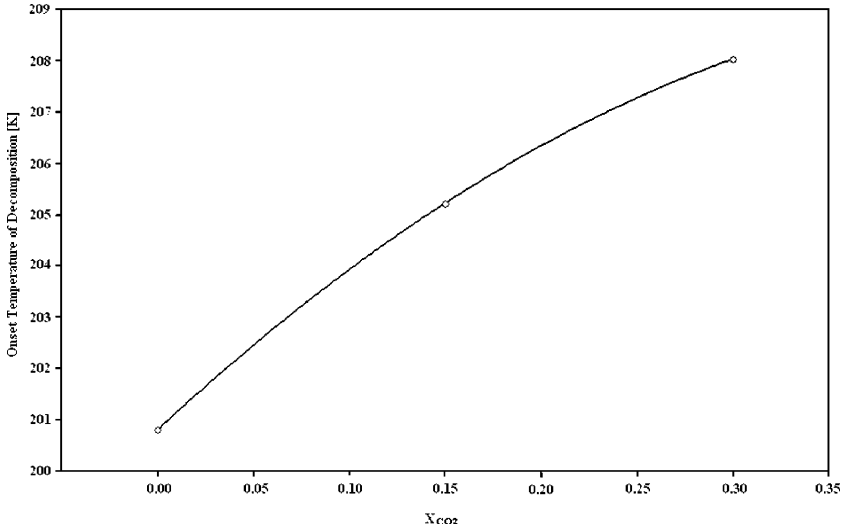

Figure 8. Onset temperatures of decomposition depending on CO_2 content.

TABLE 6: Hydrate Composition, Molar Mass, and Molar Dissociation Enthalpies

	hydrate composition				M_{GH}	$\Delta h_d'$	
sample and structure	CH_4	CO_2	C_2H_6	C_3H_8	$n = 6$ (g/mol)	$h \rightarrow i + g$ (kJ/mol)	$h \rightarrow l + g$ (kJ/mol)
mixture 1 sI	1.000				124.0	15.5	51.6
mixture 2 sI[a]	0.850	0.150			128.2	17.3	53.4
mixture 3 sI[a]	0.700	0.300			132.4	16.9	53.0
mixture 4 sII[b]	0.714		0.071	0.214	131.1	38.3	74.4
mixture 5 sI[b]	0.990		0.010		124.1	32.6	68.7
mixture 5 sII[b]	0.942		0.017	0.041	125.4	33.2	69.3

[a] Obtained through Raman spectroscopic measurements. [b] Predicted with CSMGEM.

2 and 7) has an average value of 192.5 K with a deviation of about ±1 K. This corresponds well with results obtained by Falabella.[19]

Raman spectroscopic measurements performed on the CH_4-CO_2 hydrates showed that the CO_2 content within the hydrate is three times the CO_2 content in the feed gas. Hence, the gas hydrates formed from Mixture 2 consist of approximately 15% CO_2, whereas the gas hydrates formed from Mixture 3 contain about 30% CO_2. The results of T_0 obtained for Mixtures 2 and 3 show that T_0 increases with increasing CO_2 content. As can be seen in the temperature vs CO_2 content (%) plot in Figure 8, this relationship is nonlinear. This trend corresponds well to literature data representing the decomposition of gas hydrate into water and gas.[20]

The concept of guest-to-cavity size ratio,[2] as it was presented in the Introduction, can be used to explain the increase in temperature stability of CH_4-CO_2 hydrates with an increasing CO_2 fraction. CH_4 molecules are known to occupy small as well as large cages of structure I hydrates, whereas CO_2, in general, only occupies the large cavities in this structure.[2] However, the guest-to-cavity size ratios (GCR) for the methane and carbon dioxide molecules indicate that CO_2 (GCR = 0.834) stabilizes the large cage better than CH_4 (GCR = 0.744; see also Table 2). Therefore, it can be concluded that the more CO_2 molecules are encaged in the large cages of the sI hydrate lattice instead of CH_4, the more stable the lattice becomes. Consequently, the temperature stability of CO_2-CH_4 hydrates might reach a maximum when all of the large cavities are filled with CO_2.

To draw conclusions from the results obtained for the gas hydrates formed from Mixtures 4 and 5, knowledge about the composition of the hydrate phase is required. Because no experimental data on the hydrate composition is available in this case, the interpretations are based on gas hydrate compositions calculated at the Colorado School of Mines using the hydrate prediction program CSMGEM (Keith Hester, Center of Hydrate Research, Colorado School of Mines, personal conversation). The calculated gas hydrate compositions are presented in Table 6. As can be seen, T_0 generally increases with increasing C_2H_6 fraction, which is consistent with the concept of guest-to-cavity size ratio. The addition of ethane to the hydrate forming methane has a lesser effect on T_0 than the addition of small amounts of propane, which results in a more dramatic change in stability. Therefore, it is very likely that the addition of <1% C_2H_6 has no measurable effect on the temperature stability of the hydrate within the experimental errors.

3.2. Enthalpy of Gas Hydrate Dissociation. The peak area in Figure 9 represents the amount of heat that is consumed by the sample during transition and is, hence, proportional to the total enthalpy of dissociation (ΔH_d). The specific enthalpy is then obtained by dividing ΔH_d by the mass of hydrate in the sample. The obtained values of specific enthalpy Δh_d for all hydrate systems are presented in Table 5.

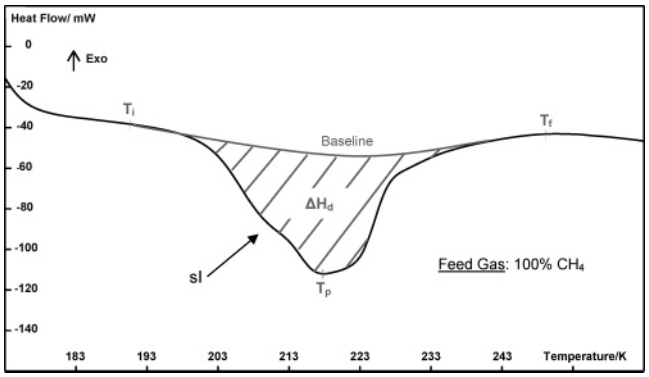

Figure 9. Determination of total enthalpy of dissociation ΔH_d of Mixture 1.

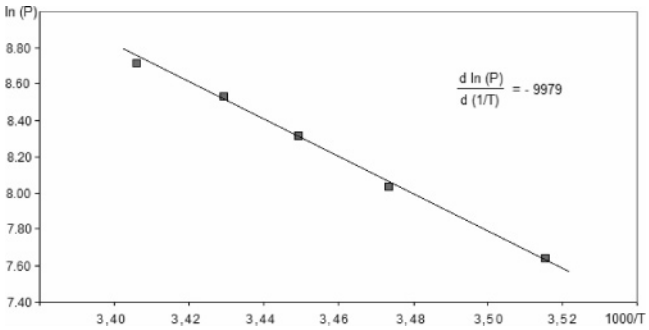

Figure 10. Clausius−Clapeyron plot of L_w-H-V data for ternary gas mixture (Mixture 4).

For a thorough interpretation, from a molecular point of view, it is helpful to convert the *specific* dissociation enthalpies Δh_d (Table 5) into *molar* enthalpies ($\Delta h_d'$ given in kJ/mol). The molar mass of gas hydrates (M_{GH}) can be calculated by the following equation:

$$M_{GH} = M_{gas} + n \cdot M_{H_2O} = \sum_i x_i \cdot M_i + n \cdot M_{H_2O} \qquad (2)$$

where n is the hydration number, M_{H_2O} represents the molar mass of water, and M_{gas} is the molar mass of the guest gas. In the case of a gas mixture, M_{gas} is the sum of the mole fractions of enclathrated gas i (x_i) times the molar mass of gas i (M_{x_i}). Here, again, the gas hydrate compositions given in Table 6 are applied. The gas hydrate compositions, molar masses, and the resulting molar enthalpies of gas hydrate dissociation are given in Table 6. For the calculations, a gas hydrate composition of six water molecules per gas molecule ($n = 6$) was assumed. This assumption was based on the determination of the water-to-gas ratio by analyzing Raman spectra of hydrate crystals as well as on calculations of the gas hydrate composition with CSMHYD and CSMGEM. The molar enthalpy of the dissociation of hydrate into gas and water, which is also given in Table 6, was obtained by adding the enthalpy of fusion of 6 mol of water to $\Delta h_d'$ (molar enthalpy of ice fusion $\Delta h_d'(H_2O) = 6.008$ kJ/mol[9]).

As can be seen, the methane hydrate has the lowest value of $\Delta h_d'$ (15.5 kJ/mol). The gas hydrates formed from mixtures of CO_2 and CH_4 show higher enthalpies. Within experimental errors for both CH_4-CO_2 compositions, $\Delta h_d'$ has the same value of about 17 kJ/mol. Gas hydrates formed from the ternary mixtures of methane, ethane, and propane show dissociation enthalpies that are twice as high as those of CH_4 or CH_4-CO_2 hydrates. For both of the hydrate structures of Mixture 5, equal dissociation enthalpies were obtained, which range between 32.6 and 33.2 kJ/mol. The $\Delta h_d'$ obtained for the decomposition of the structure II hydrate formed from Mixture 4 (38.3 kJ/mol) has the highest value of all samples. It is noticeably higher than the values attained for those gas hydrates formed from Mixture 5.

Literature values of calorimetrically determined dissociation enthalpies for the decomposition of gas hydrates into gas and either water or ice are only available for pure methane hydrates.[7,21−23] It should be noted that the calculated results for $\Delta h_d'$ in Table 6 represent only rough estimations. However, the estimated values of $\Delta h_d'$ for the transition of the methane hydrates into ice and gas are the same order of magnitude as results obtained by Handa.[7]

Figure 10 shows a Clausius−Clapeyron plot depicting gas hydrate phase equilibrium data obtained by Schicks et al.[14] for gas hydrates formed from a ternary gas mixture composed of 90% methane, 5% ethane, and 5% propane (Mixture 4). Applying the Clausius−Clapeyron equation and taking 1 as the compressibility, $\Delta h_d'$ has a value of approximately 82 kJ/mol, which is almost the same order of magnitude as the result obtained for the hydrate synthesized from Mixture 4 (74.4 kJ/mol for decomposition in gas and water; see also Table 6).

As was mentioned before, in all gas hydrate phases investigated in this study, both small and large cavities of each hydrate structure can be potentially filled with a guest molecule. Therefore, similar hydration numbers (n) might be assumed for the gas hydrates of all samples, thus indicating almost the same number of water molecules per guest molecule. The portion of the dissociation enthalpy resulting from the hydrogen bonds of *1 mol* of $M\cdot(H_2O)_n$ is therefore assumed to be equal for all gas hydrate phases investigated. As a result, the different values obtained for the dissociation enthalpies of the samples must be a consequence of factors influencing the heat of hydrate dissociation other than hydrogen bonding.

The enthalpy of dissociation reflects the magnitude of stabilization because of the interactions between guest and host. Because in all the gas hydrate systems investigated the small cavities are exclusively filled with methane, differences in dissociation enthalpies of the various samples are determined by the occupants of the large cages. Comparison of the results (Table 5) with the guest-to-cavity size ratios given in Table 2 indicates that the values of $\Delta h_d'$ increase with increasing size of the guest molecules or rather with increasing guest-to-cavity size ratios for the guests of the large cages. This may provide an explanation for the similar values of $\Delta h_d'$ obtained for the sI and sII hydrates that have been synthesized from Mixture 5. For both gas hydrate phases, the ratios of guest to host diameter (C_2H_6 in $5^{12}6^2$ (GCR = 0.939) and C_3H_8 in $5^{12}6^4$ (GCR = 0.943); Table 2) are almost equal and furthermore noticeably higher than those for CH_4 or CO_2. Therefore, it could be possible that the *molar* enthalpy of dissociation of gas hydrates almost fully occupied is independent of the hydrate structure but fixed by the guest-to-cavity size ratio of its guests.

Applying the Clausius−Clapeyron theory, Sloan and Fleyfel[10] concluded that the heat of dissociation should be, within size constraints, independent of type and concentration of the mixed guest gas. This hypothesis is supported by the results obtained for the gas hydrates formed from gas mixtures containing CH_4 and CO_2. Although both gas hydrates contain different concentrations of CO_2, both samples have almost the same dissociation enthalpy. The same would have been expected from the structure II hydrates of Mixtures 4 and 5. Both gas hydrates are assumed to consist of methane, ethane, and propane with higher C_2H_6 and C_3H_8 contents in Mixture 4. Despite their equal components, both samples have significantly different values of $\Delta h_d'$. This is contradictory to the hypothesis proposed by Sloan and Fleyfel that most multicomponent gas hydrates containing appreciable amounts of methane and propane should have essentially the same molar dissociation enthalpy.[10] Nevertheless, this might be explained by regarding the dependence of $\Delta h_d'$ on the guest-to-cavity size ratios and the cavity occupation. As the content of larger molecules in a hydrate forming gas phase increases, the number of large cages occupied with methane decreases, thus approving the enthalpy. The differences between the guest-to-cavity size ratio of methane and the guest-to-cavity size ratio of the respective large molecule (Δ_{ratio}) when occupying the large cavities are given in Table 7.

From these values, it can be concluded that the change in guest-to-cavity size ratio is more significant when a CH_4 molecule, which occupies a $5^{12}6^4$ cavity in a structure II hydrate,

TABLE 7: Difference between Guest-to-Cavity Size Ratios

guest	cavity	ratio	Δ_{ratio}
CH_4	$5^{12}6^2$	0.744	0.000
CO_2	$5^{12}6^2$	0.834	0.090
CH_4	$5^{12}6^4$	0.655	0.000
C_2H_6	$5^{12}6^4$	0.826	0.171
C_3H_8	$5^{12}6^4$	0.943	0.288

is replaced by a C_2H_6 or C_3H_8 molecule than if a methane molecule, which is encaged in a $5^{12}6^2$ cavity in a structure I hydrate, is replaced by a CO_2 molecule. Therefore, it must be assumed that in the case of the $CH_4 + CO_2$ hydrates the change in dissociation enthalpy, with increasing CO_2 content, is of minor significance or even negligible within experimental errors. However, in the case of the $CH_4-C_2H_6-C_3H_8$ hydrates the change in enthalpy with an increasing content of large molecules, especially propane, is assumed to be more noticeable, which was reflected by the results of this work.

4. Summary and Conclusion

DSC in combination with XRPD was successfully applied to determine the enthalpies and onset temperatures of decomposition into ice and gas of both synthetic single- and multicomponent gas hydrates. The gas hydrates were formed from pure methane as well as methane−carbon dioxide and methane−ethane−propane mixtures. The hydrate-forming gas mixtures used in this study were chosen so that the small cavities of the resulting gas hydrates were exclusively filled with methane, whereas the occupancies of the large cavities changed with varying gas composition. Thus, changes in molar enthalpies and onset temperatures could be observed with respect to the occupation of the large cavities. The onset temperature of decomposition of both sI and sII hydrates increases with an increasing number of guest molecules larger than methane occupying the large cavities. It was seen in the results that, when the difference in guest-to-cavity size ratio between the replaced methane and the replacing guest molecule is more significant, the molar enthalpy increases with increasing number of guest molecules larger than methane occupying the large cages.

Acknowledgment. We thank Keith Hester from the Center of Hydrate Research at the Colorado School of Mines for the CSMGEM calculations of the gas hydrate compositions, which were of great help in terms of interpreting the data. The German GEOTECHNOLOGIEN program of BMBF and DFG provided funding for this work through Research Grant 03G0605A. This is publication No. GEOTECH-280 of the GEOTECHNOLOGIEN program.

References and Notes

(1) Kvenvolden, K. A. *Rev. Geophys*. **1993**, *31*, 173.

(2) Sloan, E. D. *Clathrate Hydrates of Natural Gases*, 2nd ed.; Marcel Dekker: New York, 1998.

(3) de Forcrand, R. *Comptes Rendus* **1902**, *135*, 959.

(4) Long, J. P. Gas Hydrate Formation Mechanism and Kinetic Inhibition. PHD Thesis, Colorado School of Mines, Golden, CO, 1994.

(5) Davidson, D. W.; Desando, M. A.; Gough, S. R.; Handa, Y. P.; Ratcliff, C. I.; Ripmeester, J. A.; Tse, J. S. *J. Inclusion Phenom.* **1987**, *5*, 219.

(6) Handa, Y. P. Calorimetric Studies of Laboratory Synthesized and Naturally Occurring Gas Hydrates. In *Cryogenic Properties: Processes and Applications*, 6th Cryogenics Intersociety Symposium at the 1986 Annual Meeting of the AIChE, Miami Beach, FL, Nov 2−7, 1986; Kidnay, A. J., Hiza, M. J., Frederking, T. H. K., Kerney, P. J., Wenzel, L. A., Eds.; American Institute of Chemical Engineers: New York, 1986

(7) Handa, Y. P. *J. Chem. Thermodyn*. **1986**, *18*, 915.

(8) Yamamoru, O.; Suga, H. *J. Therm. Anal*. **1989**, *35*, 2025.

(9) Atkins, P. W. *Physikalische Chemie;* Wiley-VCH: Weinheim, Germany, 2001.

(10) Sloan, E. D.; Fleyfel, F. *Fluid Phase Equilib.* **1992**, *76*, 123.

(11) Skovborg, P.; Rasmussen, P. *Fluid Phase Equilib.* **1994**, *96*, 223.

(12) Bergmann J.; Friedel, P.; Kleeberg, R. *BGMN - A New Fundamental Parameters Based Rietveld Program for Laboratory X-ray Sources, it's Use in Quantitative Analysis and Structure Investigations;* CPD Newsletter No. 20; Commission of Powder Diffraction, International Union of Crystallography, Summer 1998, pp 5−8.

(13) Collett, T. S. *Gas Hydrate Resources of the United States;* U.S. Oil and Gas Resources on CD-ROM, USGS Digital Data Series, 1995; http://energy.cr.usgs.gov/1995OGData/Hydrates/HYDRATE.pdf.

(14) Schicks, J. M.; Naumann, R.; Erzinger, J.; Hester, K. C.; Koh, C. A.; Sloan, E. D. *J. Phys. Chem. B* **2006**, *110*, 11468.

(15) Subramanian, S.; Kini, R. A.; Dec, S. F.; Sloan, E. D. *Chem. Eng. Sci.* **2000**, *55*, 1981.

(16) Subramanian, S.; Ballard, A. L.; Kini, R. A.; Dec, S. F.; Sloan, E. D. *Chem. Eng. Sci*. **2000**, *55*, 5763.

(17) Stern, L. A.; Circone, S.; Kirby, S. H.; Durham, W. B. *J. Phys. Chem. B* **2001**, *105*, 1756.

(18) Wunderlich, B. *Thermal Analysis;* Academic Press: San Diego, CA, 1990.

(19) Falabella, B. J. *A Study of Natural Gas Hydrates*. Ph.D. Thesis, University of Massachusetts, Amherst, MA, 1975.

(20) Adisasmito, S.; Frank, R. J.; Sloan, E. D. *J. Chem. Eng. Data* **1991**, *36*, 68.

(21) Lievois, J. S. *Development of an Automated, High Pressure Heat-Flux Calorimeter and Its Application To Measure the Heat of Dissociation of Methane Hydrate*. Ph.D. Thesis, Rice University, Houston, TX, 1987.

(22) Rueff, R. M.; Sloan, E. D.; Yesavage, V. F. *AIChE J*. **1988**, *34*, 1468.

(23) Kang, S. P.; Lee, H.; Ryun, B. J. *J. Chem. Thermodyn*. **2001**, *33*, 513.